Effects of higher-order fluctuations on the bulk and surface properties of quantum droplets in a heteronuclear Bose-Bose mixture

Abdelâali Boudjemâa ⬤* and Nadia Guebli ⬤

Department of Physics, Faculty of Exact Sciences and Informatics,
Hassiba Benbouali University of Chlef P.O. Box 151, 02000, Ouled Fares, Chlef, Algeria

We discuss the bulk and surface properties of ultradilute self-bound quantum droplets in a heteronuclear Bose-Bose mixture in the presence of higher-order quantum and thermal fluctuations. Within the realm of the Hartree-Fock-Bogoliubov theory, we calculate beyond the Lee-Huang-Yang corrections to the ground-state energy, the droplet equilibrium density, the surface tension, and the critical number of particles. Our predictions are compared with recent diffusion Monte Carlo simulation and density functional theory method and excellent agreement is found. We address in addition the effects of temperature on the formation and on the robustness of the heteronuclear self-bound mixtures.

I. INTRODUCTION

Since the spectacular prediction of self-bound droplets in ultracold quantum gases in 2015 by Petrov [1], intensive investigations have been carried out in the past years, both to explain the initial observations and to predict new phenomena (see, for review, Refs. [2–4] and references therein). Such ultradilute quantum liquids originate from the competition between mean-field attraction and beyond-mean-field repulsive Lee-Huang-Yang (LHY) fluctuations.

The ability to control contact interactions using Feshbach resonance allows the experimental achievement of quantum self-bound droplets in the homonuclear Bose mixtures of ^{39}K, both in the presence of an external potential [5,6] and in three-dimensional (3D) free space [7]. Collision between droplets enables to investigate the dynamical properties of self-bound systems and to observe the crossover between compressible and incompressible regimes [8]. The dynamics and the statics of quantum droplets in binary Bose-Einstein condensates (BECs) with short-range interactions can be governed by the extended Gross-Pitaevskii equation based on the Petrov prescription [1], and beyond the Petrov theory [9–12]. Quantum Monte Carlo (QMC) method simulations have been performed [13,14] in order to unveil the role played by the higher-order quantum fluctuations for the description of the 3D self-bound Bose mixtures realized in recent experiments. However, as shown by the above experimental works [7,8], the homonuclear mixtures of ^{39}K lead to the formation of short-lived droplets (few milliseconds $\sim$8 ms) due to the strong three-body losses, which prohibit the observation of the self-evaporation mechanism predicted first in Ref. [1].

On the other hand, the creation of heteronuclear quantum droplets in an attractive bosonic mixture of ^{41}K $-$ ^{87}Rb and ^{23}Na $-$ ^{87}Rb have been reported most recently in Refs. [15,16]. Their properties have been studied using the

diffusion Monte Carlo (DMC) method and density functional theory (DFT) [17]. In contrast to the homonuclear droplets, the heteronuclear self-bound liquids are very dilute since they are characterized by lower densities. They are stable long-lived structures (about three times longer than the lifetime of ^{39}K droplets). The longer lifetime and the lower three-body recombination of this exotic liquid mixture allows to observe more complex phenomena, such as the self-evaporation of the droplet [1], the characterization of the incompressible regime [15], and the creation of larger droplets [17].

In this paper, we study the properties of free-space self-bound quantum liquid droplets in heteronuclear Bose-Bose mixtures of ^{41}K $-$ ^{87}Rb [15] in the presence of higher-order quantum fluctuations. To this end, we use our Hartree-Fock-Bogoliubov (HFB) theory [11,12,18,19] that can go beyond the LHY description. It can self-consistently evaluate the quantum and thermal fluctuations stemming from the normal and anomalous correlations generalizing all existing models in the literature, such as the Bogoliubov theory [1], and the extended Gross-Pitaevskii equation [1,6,7]. The intriguing coupling between the order parameter, the normal and anomalous fluctuations makes the HFB a promising approach for exploring quantum self-bound droplets in dipolar [19] and nondipolar Bose-Bose mixtures [11,12,18] at both zero and finite temperatures. Furthermore, the HFB theory is able to explain existing experimental and QMC results [11,12,20].

We calculate, in particular, the ground-state energy, the equilibrium density, the surface tension, the critical number of particles, and compare them with available DMC and DFT data. It is found that our results excellently agree with the predictions of DMC simulations [17]. This shows the pertinence of our theory in capturing higher-order quantum correlation effects. We then extend our calculations to finite temperature and study the thermal dependence of the self-bound droplet. We compute, in particular, the free energy and the critical temperature above which the droplet evaporates. It is pointed out that the self-bound droplet remains robust even for

---

*a.boudjemaa@univ-chlef.dz

relatively large thermal fluctuations in contrast to the homonuclear case. This might lead to a possible long-lived droplet. At temperatures higher than the critical temperature, the droplet becomes unstable and entirely evaporates.

The rest of the paper is structured as follows. In Sec. II, we introduce the HFB model for heteronuclear Bose mixtures. In Secs. III–V our theoretical results for the ground-state energy, the equilibrium density, the surface tension, and the critical atom numbers are presented and compared with the recently available DMC data. Section VI describes the thermal effects on the stabilization mechanism of the heteronuclear self-bound droplet. We accurately calculate the free energy and the critical temperature of the droplet. Section VII is dedicated to the conclusions and outlooks.

II. MODEL

We consider homogeneous heteronuclear two-component BECs with masses m_1 and m_2 in a volume V and a total number of bosons $N = N_1 + N_2$. The dynamics of this system including the effect of quantum and thermal fluctuations is governed by the coupled time-dependent HDB (TDHFB) equations which can be written as [11,12,18–20]

$$i\hbar \frac{d\Phi_j}{dt} = \left(h_j^{sp} + g_j n_j + g_{12} n_{3-j} + \delta\mu_{j\text{LHY}} \right)\Phi_j, \quad (1)$$

where $h_j^{sp} = -(\hbar^2/2m_j)\Delta - \mu_j$ is the single-particle Hamiltonian, μ_j is the chemical potential of each component ($j = 1, 2$), $\delta\mu_{j\text{LHY}}(\mathbf{r})\Phi_j(\mathbf{r}) = g_j[\tilde{n}_j(\mathbf{r})\Phi_j(\mathbf{r}) + \tilde{m}_j(\mathbf{r})\Phi_j^*(\mathbf{r})]$ is the relevant LHY term, which is obtained self-consistently, $\hat{\bar{\psi}}_j(\mathbf{r}) = \hat{\psi}_j(\mathbf{r}) - \Phi_j(\mathbf{r})$ is the noncondensed part of the field operator with $\Phi_j(\mathbf{r}) = \langle\hat{\psi}_j(\mathbf{r})\rangle$, $n_{cj} = |\Phi_j|^2$ is the condensed density, $\tilde{n}_j = \langle\hat{\bar{\psi}}_j^\dagger\hat{\bar{\psi}}_j\rangle$ is the noncondensed density, $\tilde{m}_j = \langle\hat{\bar{\psi}}_j\hat{\bar{\psi}}_j\rangle$ is the anomalous correlation, and $n_j = n_{cj} + \tilde{n}_j$ is the total density of each species. In 3D Bose mixtures, the intra- and interspecies coupling strengths are given, respectively, by $g_j = (4\pi\hbar^2/m_j)a_j$ and $g_{12} = g_{21} = 2\pi\hbar^2(m_1^{-1} + m_2^{-1})a_{12}$ with a_j and a_{12} being the intraspecies and the interspecies scattering lengths.

The elementary excitations of a homogeneous Bose mixture, can be computed by linearizing Eq. (1) via the generalized random-phase approximation: $\Phi_j = \sqrt{n_{cj}} + \delta\Phi_j$, where $\delta\Phi_j(\mathbf{r}, t) = u_{jk}e^{i\mathbf{k}\cdot\mathbf{r}-i\varepsilon_k t/\hbar} + v_{jk}e^{i\mathbf{k}\cdot\mathbf{r}+i\varepsilon_k t/\hbar} \ll \sqrt{n_{cj}}$ [18,19]. The solution of the obtained second-order-coupled TDHFB–de Gennes equations provides the following expressions for the quasiparticle amplitudes [18],

$$u_{+k}, v_{+k} = \frac{1}{2}\left(\sqrt{\frac{\varepsilon_{+k}}{E_{1k}}} \pm \sqrt{\frac{E_{1k}}{\varepsilon_{+k}}} \right), \quad (2a)$$

$$u_{-k}, v_{-k} = \frac{1}{2}\left(\sqrt{\frac{\varepsilon_{-k}}{E_{2k}}} \pm \sqrt{\frac{E_{2k}}{\varepsilon_{-k}}} \right), \quad (2b)$$

and correction terms to the Bogoliubov excitations energy,

$$\varepsilon_{k\pm} = \sqrt{\frac{\varepsilon_{1k}^2 + \varepsilon_{2k}^2}{2} + \sqrt{\frac{\left(\varepsilon_{1k}^2 - \varepsilon_{2k}^2\right)^2}{4} + 4g_{12}^2 n_1 n_2 E_{1k} E_{2k}}}, \quad (3)$$

where $\varepsilon_{jk} = \sqrt{E_{jk}^2 + 2E_{jk}\bar{g}_j n_{cj}}$ are the Bogoliubov spectra for each species and $E_{jk} = \hbar^2 k^2/(2m_j)$ is the energy of free particle in each component. Here, the density-dependent coupling constants $\bar{g}_j = g_j(1 + \tilde{m}_j/n_{cj})$ have been introduced in order to guarantee the gaplessness of the spectrum [11,18]. The Bogoliubov dispersions (3) exhibit a phononlike linear dependence on k in the long-wavelength limit $\varepsilon_{k\pm} = \hbar c_{s\pm} k$, where

$$c_{s\pm}^2 = \frac{1}{2}\left(c_{s1}^2 + c_{s2}^2 \pm \sqrt{\left(c_{s1}^2 - c_{s2}^2\right)^2 + 4c_{s12}^2} \right)$$

are the sound velocities with $c_{sj} = \sqrt{\bar{g}_j n_{cj}/m_j}$ and $c_{s12} = \sqrt{g_{12}^2 n_1 n_2/m_1 m_2}$ being the sound velocities for the individual components. The stability condition requires: $c_{s1}c_{s2} > c_{s12}^2$. This implies

$$\bar{g}_1\bar{g}_2 > g_{12}^2, \quad \text{or} \quad g_1\left(1 + \frac{\tilde{m}_1}{n_{c1}}\right)g_2\left(1 + \frac{\tilde{m}_2}{n_{c2}}\right) > g_{12}^2, \quad (4)$$

meaning that the anomalous fluctuations are necessary for the stability of the mixture at both zero and nonzero temperatures.

At zero temperature, the noncondensed density is defined as: $\tilde{n} = V^{-1}\sum_{\mathbf{k}}\sum_\pm v_{\pm k}^2$ [18]. We then replace the wave-vector sum by an integral $V^{-1}\sum_{\mathbf{k}} \rightarrow (1/2\pi^2)\int_0^\infty dk\, k^2$. After integrating over k, we obtain

$$\tilde{n} = \frac{2\sqrt{2}}{3}n_1\sqrt{\frac{n_1 a_1^3}{\pi}}\left(1 + \frac{\tilde{m}_1 - \tilde{n}_1}{n_1}\right)^{3/2}\mathcal{U}(z, x, y), \quad (5)$$

where $\mathcal{U}(z, x, y) > 1$ is a dimensionless function. For $z = 1$, it simplifies to $\mathcal{U}(1, x, y) = \sum_\pm[1 + y \pm \sqrt{(1 - y)^2 + 4xy}]^{3/2}/2\sqrt{2}$ [11,18].

The anomalous density, which describes correlations between bosonic pairs, is given by $\tilde{m} = V^{-1}\sum_{\mathbf{k}}\sum_\pm u_{\pm k}v_{\pm k}$ [18]. It strongly depends on the interparticle interactions. Summing over all states would cause ultraviolet divergences in the anomalous density. To circumvent, such a divergence arising from the use of the contact interactions, we should introduce the renormalized coupling constants [1,11,21],

$$g_j(\mathbf{k}) = g_j + g_j^2\int\frac{d\mathbf{k}}{(2\pi)^3}\frac{1}{2E_k}, \quad (6a)$$

$$g_{12}(\mathbf{k}) = g_{12} + g_{12}^2\int\frac{d\mathbf{k}}{(2\pi)^3}\frac{1}{2E_k}. \quad (6b)$$

After the subtraction of the ultraviolet divergent part, the renormalized anomalous density takes the form

$$\tilde{m} = -\frac{1}{2\pi^2}\int_0^\infty dk\, k^2\left[\frac{1}{\varepsilon_k} - \frac{n_j^2 g_j^2}{2E_k} - \frac{n_1 n_2 g_{12}^2}{2E_k}\right]. \quad (7)$$

This yields

$$\tilde{m} = 2\sqrt{2}\, n_1\sqrt{\frac{n_1 a_1^3}{\pi}}\left(1 + \frac{\tilde{m}_1 - \tilde{n}_1}{n_1}\right)^{3/2}\mathcal{U}(z, x, y). \quad (8)$$

Equation (8) clearly shows that $\tilde{m}$ is three times larger than $\tilde{n}$ at zero temperature, so the omission of the anomalous density in Bose systems is indeed an unfaithful approximation. This indicates that the anomalous density is essential in obtaining

higher-order fluctuations and, thus, in the stability of Bose mixtures [see also Eq. (4)]. Similar behavior is also present in a single BEC [23–27].

At very low temperature, the energy of the system per unit volume including higher-order quantum fluctuations reads [11]

$$\frac{E}{V} = \frac{1}{2} \sum_{j=1}^{2} g_j n_j^2 + g_{12} n_1 n_2 + \frac{E_{\text{LHY}}}{V}, \tag{9}$$

where

$$\frac{E_{\text{LHY}}}{V} = \sum_{\mathbf{k}} \sum_{\pm} \varepsilon_{\pm k} v_{\pm k}^2 \tag{10}$$

stands for the LHY corrections to the ground-state energy, which is ultraviolet divergent. To eliminate this problem, we employ again the renormalized coupling constants (6). This gives

$$\frac{E_{\text{LHY}}}{V} = \frac{16 g_1 \sqrt{a_1^3/\pi}}{15\sqrt{2}} n_1^{5/2} \left(1 + \frac{\tilde{m}_1 - \tilde{n}_1}{n_1} \right)^{5/2} f\left(\frac{m_2}{m_1}, \frac{g_{12}^2}{\bar{g}_1 \bar{g}_2}, \frac{\bar{g}_2 n_{c2}}{\bar{g}_1 n_{c1}} \right), \tag{11}$$

where $f(z, x, y) > 1$ ($z = m_2/m_1, x = g_{12}^2/\bar{g}_1\bar{g}_2, y = \bar{g}_2 n_{c2}/\bar{g}_1 n_{c1}$) is a dimensionless function. For homonuclear mixtures, $z = 1$, the function f reduces to $f(1, x, y) = \sum_{\pm}[1 + y \pm \sqrt{(1-y)^2 + 4xy}]^{5/2}/4\sqrt{2}$, thus, $f(1, 1, y) = (1 + y)^{5/2}$, and $f(1, 1, 1) = 1$ [11,18]. For $\tilde{m}_j = 0$ and $n_c \approx n$, one can reproduce the early Larsen formula [21]. In the heteronuclear case, a simple analytical expression for $f(z, x, y)$ is not accessible. According to Refs. [1,22], in the region where $x \sim 1$ (i.e., f is weakly dependent on x), the expression of the dimensionless function f is given by

$$f(z, x, y) = \frac{15}{32} \int_0^{\infty} k^2 \mathcal{F}(k, z, x, y) dk, \tag{12}$$

where

$$\mathcal{F}(k, z, x, y) = \sqrt{\frac{1}{2}\left[k^2\left(1 + \frac{y}{z}\right) + \frac{1}{4}k^4\left(1 + \frac{1}{z^2}\right)\right] + \left\{\frac{1}{4}\left[\left(k^2 + \frac{1}{4}k^4\right) - \left(\frac{y}{z}k^2 + \frac{1}{4z^2}k^4\right)\right]^2 + x\frac{y}{z}k^4\right\}^{1/2}}$$

$$+ \sqrt{\frac{1}{2}\left[k^2\left(1 + \frac{y}{z}\right) + \frac{1}{4} - k^4\left(1 + \frac{1}{z^2}\right)\right] - \left\{\frac{1}{4}\left[\left(k^2 + \frac{1}{4}k^4\right) - \left(\frac{y}{z}k^2 + \frac{1}{4z^2}k^4\right)\right]^2 + x\frac{y}{z}k^4\right\}^{1/2}}$$

$$- \frac{1+z}{2z}k^2 - (1+y) + \frac{1}{k^2}\left[1 + y^2 z + 4xy\frac{z}{1+z}\right]. \tag{13}$$

Equations (8)–(11) are self-consistent that can be solved by iteration, and whose solutions directly provide the desired corrections to the ground-state energy and fluctuations of the droplet.

From now on, we consider the case of a mixture of the hyperfine state $|F = 1, m_F = 1\rangle$ of ^{41}K as component 1, and the hyperfine state $|F = 1, m_F = 1\rangle$ of ^{87}Rb as component 2. The scattering parameters describing the intraspecies repulsion are fixed and their values are equal to $a_1 = 65a_0$ [28], and $a_2 = 100.4a_0$ [29]. Experimentally, the interspcies interaction a_{12} varies from $-80a_0$ to $-95a_0$ [15].

The result of the numerical integration of Eq. (12) for the case of ^{41}K $- ^{87}$Rb mixture ($z \simeq 2.1$) close to the mean-field collapse ($x \sim 1$) with and without higher-order corrections is displayed in Fig. 1. We see that the higher-order fluctuations may increase the function f, in particular, for large y leading to enhance the ground-state energy giving rise to affect the behavior of the droplet as we will see below.

III. BULK PROPERTIES

In this section, we analyze the bulk properties of ^{41}K $- ^{87}$Rb mixture in the droplet regime. According to the Petrov theory [1], the stability of the mixture against fluctuations requires the condition: $n_2/n_1 = \sqrt{\bar{g}_1/\bar{g}_2}$. Therefore, the energy functional becomes effectively single component, and can be written in terms of the total density $n = n_1 + n_2$ as

$$\frac{E}{N} = \frac{2\pi\hbar^2\left[2a_1 z + a_{12}\sqrt{\frac{a_1}{a_2}}z(1+z)\right]}{m_2\left(\sqrt{\frac{a_1}{a_2}}z + 1\right)^2} n^2$$

$$+ \frac{256\sqrt{\pi}\hbar^2 a_1^{5/2}}{15 m_1} \left(\frac{1 + z^{1/10}\sqrt{a_2/a_1}}{1 + \sqrt{\frac{a_1}{a_2}}z} \right)^{5/2} n^{5/2}$$

$$\times \left(1 + \frac{\tilde{m} - \tilde{n}}{n} \right)^{5/2}. \tag{14}$$
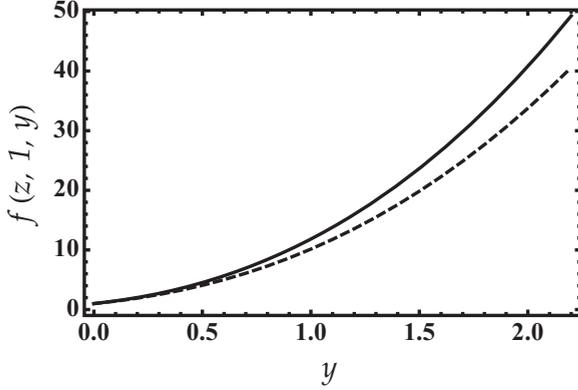
FIG. 1. The dimensionless function f from Eq. (12) for $^{41}K - ^{87}Rb$ mixture ($z \simeq 2.1$). The solid line: Our predictions. The dashed line: Without higher-order corrections.

In Fig. 2, we plot the energy (14) and compare it with theoretical predictions [1], and recent DMC energies obtained using finite-range potentials [17] for different values of the interspecies interactions a_{12}. DMC simulations were performed with two models of the interaction potential called POT-I and POT-II, which satisfy both scattering parameters, namely, the s-wave scattering length a and the effective range r_{eff}. This latter can be estimated from the knowledge of the Van der Waals coefficient, C_6 (for more details, we refer the reader to Ref. [17]).

We see that our findings agree with the theoretical predictions [1] at densities smaller than the equilibrium density, revealing the universality of our theory in such a regime. Whereas, they down-shift from the Bogoliubov results [1] at relatively higher densities due to the inclusion of the anomalous correlations (pairing effects) [11]. On the other hand, our HFB predictions are in excellent agreement with the DMC simulations [17] for the three values of a_{12}. This proves the relevance of the beyond LHY stabilization of quantum liquid droplets in heteronuclear Bose mixtures.

The equilibrium density of the droplet can be obtained by minimizing the energy. For analytical tractability, we retain only first order in $\tilde{n}$ and $\tilde{m}$. This yields

$$n_{eq} = \frac{25\pi}{4096a_1^3} \left[\frac{2 + a_{12}/a_1 \sqrt{\frac{a_1}{a_2}} z(1+z^{-1})}{\left(\sqrt{\frac{a_1}{a_2}} z + 1 \right) f(z, 1, \sqrt{\bar{g}_2/\bar{g}_1})} \right]^2. \quad (15)$$

The behavior of the equilibrium density is displayed in Fig. 3. We see that our results improve those obtained from the standard Bogoliubov approach. Another important remark is that beyond a certain critical value of a_{12}, the equilibrium density tends to zero and, hence, the liquid evaporates. The reason is that the interspecies interactions are not strong enough to balance the LHY repulsion even they are attractive, therefore, the droplet cannot preserve its self-bound character.

IV. SURFACE TENSION

The surface tension is a relevant parameter in a liquid droplet that governs its existence, stability, and equilibrium shape. In the case of quantum droplets, the kinetic energy acts

$a_{12} = -85\ a_0$
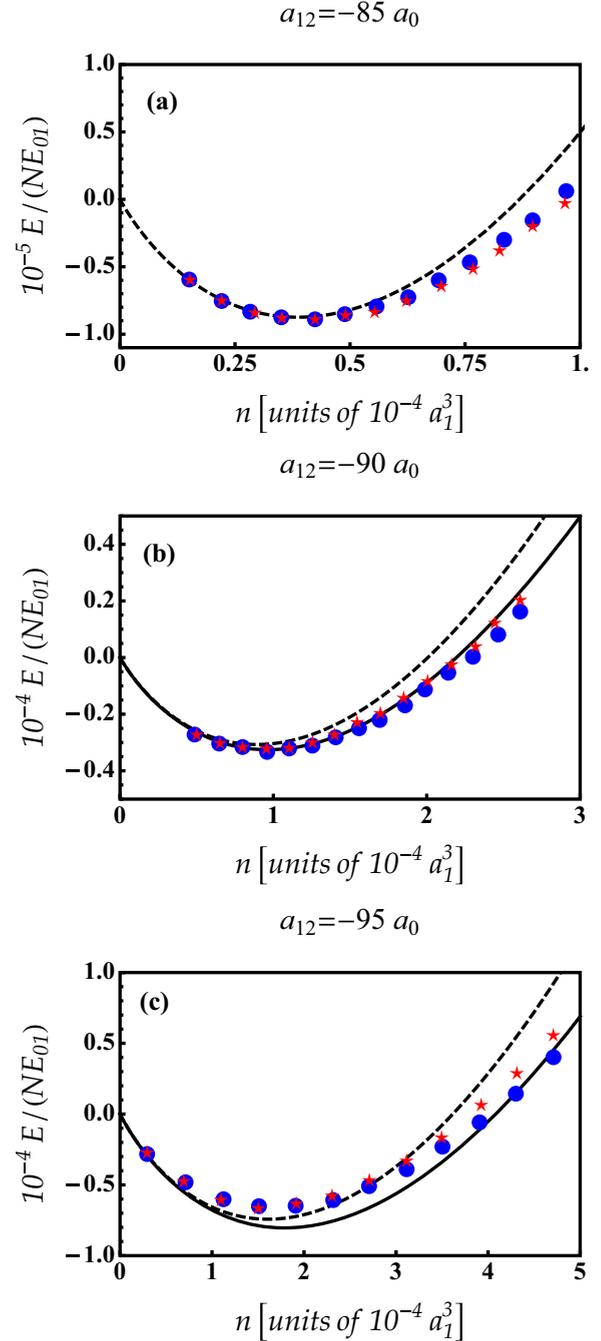
$a_{12} = -90\ a_0$

$a_{12} = -95\ a_0$

FIG. 2. Ground-state energy $E/(NE_{01})$ as a function of the density (na_1^3) for different values of a_{12}. (a) $a_{12} = -85a_0$, (b) $a_{12} = -90a_0$, and (c) $a_{12} = -95a_0$. Dashed lines correspond to the standard Bogoliubov theory [1]. Solid lines correspond to our results up to first-order corrections of quantum fluctuations. Circles represent the DMC results corresponding to POT-I model [17]. Stars represent the DMC results corresponding to POT-II model [17]. Here $E_{01} = \hbar^2/(2m_1a_1^2)$.

as a surface tension, providing an extra energy that depends on the density gradient at the surface. The surface tension of the planar interface consists of assuming an infinite homogeneous system along the xy plane, and we study the density profile along the z axis (i.e., we use a slab geometry) [17]. Let us
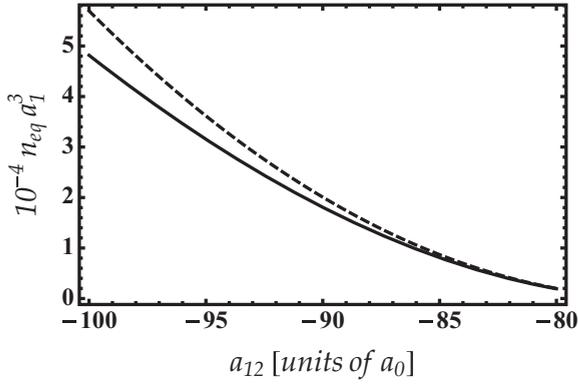
FIG. 3. Equilibrium density of the self-bound droplet n_{eq} as a function of the interspecies scattering length a_{12}/a_0. Solid lines correspond to our results from Eq. (15). Dashed lines correspond to the theory of Ref. [1].

rewrite the energy density E of the mixture in terms of density n_1 using the assumption $n_2/n_1 = \sqrt{g_1/g_2}$ [1],

$$E = \alpha \frac{(\nabla \sqrt{n_1})^2}{n_1} + \beta n_1^2 + \gamma n_1^{5/2} (1 + \lambda \sqrt{n_1})^{5/2}, \quad (16)$$

where

$$\alpha = (\hbar^2/8m_1^2)(1 + z^{-1}\sqrt{g_1/g_2}),$$

$$\beta = g_1 + g_{12}\sqrt{g_1/g_2},$$

$$\gamma = \frac{8}{15\pi^2} \left(\frac{m_1}{\hbar^2}\right)^{3/2} g_1^{5/2} f\left(z, 1, \frac{\bar{g}_2}{\bar{g}_1}\right),$$

$$\lambda = 1 + \frac{4}{3\sqrt{\pi}} \left(\frac{1 + \sqrt{a_2 z^{-1}/a_1}}{1 + \sqrt{a_2 z^{-1}/a_1}}\right)^{3/2}.$$

The surface tension of the planar interface represented by the energy functional (16) can be computed using the integral [17,30],

$$\sigma = 2 \int_0^{n_{eq}} dn_1 \sqrt{\alpha \left[\beta n_1 + \gamma n_1^{3/2}(1 + \lambda\sqrt{n_1})^{5/2} - \mu_0\right]}, \quad (17)$$

where $\mu_0 = \beta n_{n_{eq}} + \gamma n_{n_{eq}}^{3/2}(1 + \lambda \sqrt{n_{n_{eq}}})^{5/2}$ is the chemical potential of the droplet, evaluated at the equilibrium density n_{eq}.

The corresponding density profile can be obtained via

$$z = z_0 + \int_{n_{eq}/2}^{n} dn' h(n'), \quad (18)$$

where

$$h(n) = -\sqrt{\frac{\alpha}{n} [\beta n^2 + \gamma n^{5/2}(1 + \lambda\sqrt{n})^{5/2} - \mu_0 n]},$$

with $n \in [0, n_{eq}]$. Here, the minus sign indicates that the density profile is decreasing from bulk to vacuum.

Evidently, Eqs. (17) and (18) for the surface tension and the density profile extend naturally those of Refs. [17,30]. The results of their numerical integration are shown in Figs. 4 and 5.

Figure 4 illustrates the comparison between the obtained surface tension (17) and the QMC-based functional POT-I of Ref. [17]. The surface tension axis is on the logarithmic scale

in order to well emphasize its rate of change as a function of the interspecies interactions. We observe that our findings agree well with QMC calculations [17] in the whole range of a_{12}/a_0.
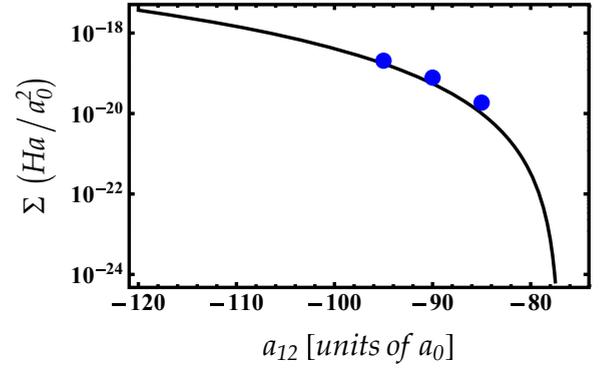
FIG. 4. Surface tension (on the logarithmic scale) as a function of the interspecies scattering length a_{12}/a_0. The solid line corresponds to our results. Circles represent the QMC results corresponding to the POT-I model [17].
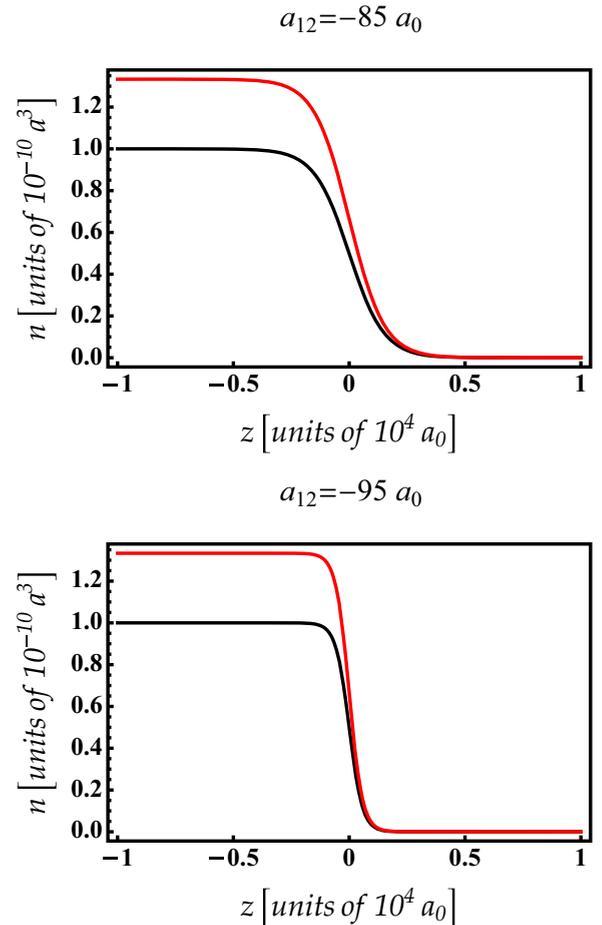
FIG. 5. Density profile along the z direction for different values of the interspecies scattering length a_{12}/a_0. The red lines: Our predictions. The black lines: Standard results without higher-order corrections.
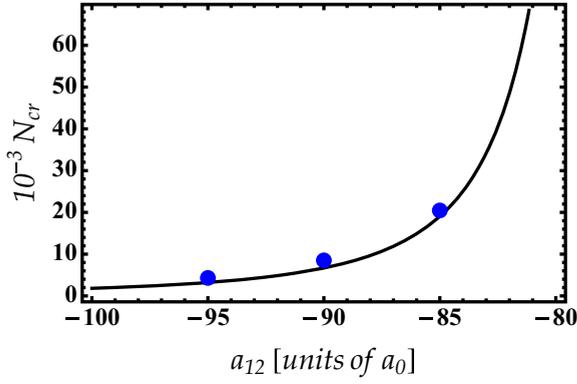
FIG. 6. Critical atom number N_{cr} as a function of the interspecies scattering length a_{12}/a_0. The solid line corresponds to our results. The circles represent the QMC results corresponding to the POT-I model [17].

The density profiles (18) for different values of a_{12} are reported in Fig. 5. We see that the presence of the higher-order effects leads to decrease the density of the droplet as foreseen above.

V. CRITICAL NUMBER OF ATOMS

To determine the critical number of atoms N_{cr}, we can use a variational method. The assumed density profile of the first component of the mixture takes the form: $n_1(r) = N_1 e^{-r^2/\sigma^2}/(\pi^{3/2}\sigma^3)$. Inserting this ansatz into Eq. (16), the effective single-component energy per particle turns out to be given

$$\frac{E}{N_1} = \frac{6\alpha}{\sigma^2} + \frac{\beta}{(2\pi)^{3/2}}\frac{N_1}{\sigma^3} + \int dr\, \gamma n_1^{5/2}(1 + \lambda\sqrt{n_1})^{5/2}. \quad (19)$$

For a fixed value of a_{12}, we are interested in the pair of parameters $(\sigma_0, N_{1,cr})$ for which the conditions $\partial(E/N_1)/\partial\sigma = 0$ (for a minimum) and $E/N_1 = 0$ (gives the line separating stable droplets with negative total energy from unstable ones with positive energy) must be fulfilled [17].

In the presence of higher-order fluctuations, the above system cannot be solved analytically. Therefore, we solve it numerically with respect to σ, for the critical total number of atoms $N_{cr} = N_{1,cr}(1 + \sqrt{g_1/g_2})$. We, then, compare our results with QMC data of Ref. [17]. Figure 6 shows that the critical atom number obtained from our HFB theory is in perfect agreement with the QMC simulations of Ref. [17] due to the effects of higher-order quantum correlations.

VI. THERMAL DESTABILIZATION

In this section, we discuss the thermal destabilization of quantum droplets in heteronuclear Bose-Bose mixtures of $^{41}\text{K} - ^{87}\text{Rb}$.

In the frame of the HFB formalism, the free energy can be written as [18,20]

$$F = E + \frac{T}{2\pi^2}\int k^2 dk \sum_{\pm} \ln\left(\frac{2}{\sqrt{I_{k\pm}}+1}\right), \quad (20)$$
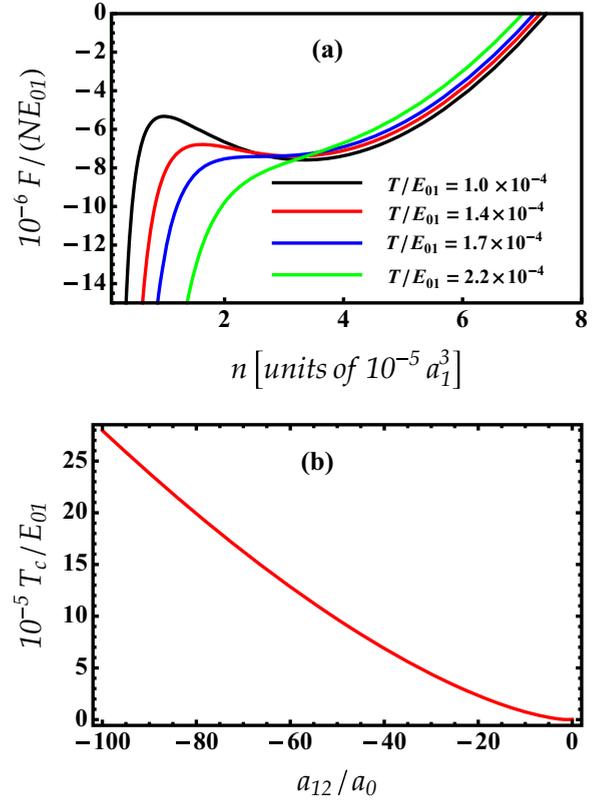
FIG. 7. (a) Free energy as a function of the density (na_1^3) for $a_{12} = -85a_0$ at different values of temperature T/E_{01}. (b) Critical temperature as a function of the interspecies scattering length a_{12}/a_0.

where $I_{k\pm} = \coth^2(\varepsilon_{k\pm}/2T)$. At low temperature, the main contribution to integral (20) comes from the phonon branch. This yields

$$\frac{F}{V} = \frac{E}{V} - \frac{\pi^2}{90}\frac{T^4}{\hbar^3}\sum_{\pm}\frac{1}{c_{s\pm}^3}, \quad (21)$$

which can be rewritten as

$$\frac{F}{N} = \frac{E}{N} - \frac{\sqrt{2}m_1^{3/2}(g_1 n_1)^{5/2}}{45\pi^2\hbar^3}\left(1 + \frac{\tilde{m}_1 - \tilde{n}_1}{n_1}\right)^{-3/2}$$
$$\times f(z, x, y)^{-1/2}\left(\frac{\pi T}{g_1 n_1}\right)^4, \quad (22)$$

where E/N is given in Eq. (14). The presence of the normal and anomalous fluctuations in Eq. (22) not only ensures the convergence of the free energy, but also provides higher-order corrections, which may shift the critical temperature of the self-bound droplet.

We show in Fig. 7(a) the free energy up to second-order computed at different values of temperatures. It is found that below a certain critical temperature $T < T_c \simeq 1.7E_{01}$, the free energy features a local maximum, corresponding to the formation of an unstable droplet, and a local minimum supporting a higher-density stable self-bound solution. The two solutions disappear at the critical temperature $(T = T_c \simeq 1.7E_{01})$, indicating that the liquidlike droplet starts to evaporate. Importantly, this critical temperature is somehow higher than that predicted for the homonuclear droplet where

T_c is comparable with the ground-state energy of the liquid [9–11,20], giving rise to the formation of long-lived droplets. This fascinating feature enables the observation of the self-evaporation mechanism. Augmenting further the temperature ($T > T_c$), the self-bound state becomes unstable and, then, completely evaporates eventually. Likewise, the homonuclear case, the critical temperature T_c of the heteronuclear droplet is also decreasing with the interspecies interactions as shown in Fig. 7(b).

VII. CONCLUSIONS

In this paper, we deeply investigated the bulk and the surface properties of the $^{41}K - ^{87}Rb$ quantum liquid mixture in the presence of higher-order quantum and thermal corrections. The ground-state energy, the droplet equilibrium density, the surface tension, and the critical number of particles have been computed using the HFB theory. We compared our results with recent predictions of DMC simulation and the DFT method and excellent agreement is found. At finite temperature, we revealed that a robust droplet can survive even for relatively large temperature compared to the homonuclear self-bound droplets. The results acquired from this research could uncover valuable insights and support future experiments for many interesting phenomena, such as the self-evaporation and larger droplets.

[1] D. S. Petrov, Phys. Rev. Lett. **115**, 155302 (2015).

[2] Z.-H. Luo, W. Pang, B. Liu, Y.-Y. Li, and B. A. Malomed, Front. Phys. **16**, 32201 (2021).

[3] F. Böttcher, J.-N. Schmidt, J. Hertkorn, K. Ng, Graham, M. Guo, T. Langen, and T. Pfau, Rep. Prog. Phys. **84**, 012403 (2021).

[4] M. Guo and T. Pfau, Front. Phys. **16**, 32202 (2021).

[5] C. R. Cabrera, L. Tanzi, J. Sanz, B. Naylor, P. Thomas, P. Cheiney, and L. Tarruell, Science **359**, 301 (2018).

[6] P. Cheiney, C. R. Cabrera, J. Sanz, B. Naylor, L. Tanzi, and L. Tarruell, Phys. Rev. Lett. **120**, 135301 (2018).

[7] G. Semeghini, G. Ferioli, L. Masi, C. Mazzinghi, L. Wolswijk, F. Minardi, M. Modugno, G. Modugno, M. Inguscio, and M. Fattori, Phys. Rev. Lett. **120**, 235301 (2018).

[8] G. Ferioli, G. Semeghini, L. Masi, G. Giusti, G. Modugno, M. Inguscio, A. Gallemí, A. Recati, and M. Fattori, Phys. Rev. Lett. **122**, 090401 (2019).

[9] M. Ota and G. E. Astrakharchik, SciPost Phys. **9**, 020 (2020).

[10] H. Hu, J. Wang, X.-J. Liu, Phys. Rev. A **102**, 043301 (2020).

[11] N. Guebli and A. Boudjemâa, Phys. Rev. A **104**, 023310 (2021).

[12] A. Boudjemâa, Sci. Rep. **11**, 21765 (2021).

[13] C. Staudinger, F. Mazzanti, and R. E. Zillich, Phys. Rev. A **98**, 023633 (2018).

[14] V. Cikojevic, L. V. Markic, G. E. Astrakharchik, and J. Boronat, Phys. Rev. A **99**, 023618 (2019).

[15] C. D'Errico, A. Burchianti, M. Prevedelli, L. Salasnich, F. Ancilotto, M. Modugno, F. Minardi, and C. Fort, Phys. Rev. Res. **1**, 033155 (2019).

[16] Z. Guo, F. Jia, L. Li, Y. Ma, J. M. Hutson, X. Cui, and D. Wang, Phys. Rev. Res. **3**, 033247 (2021).

[17] V. Cikojević, E. Poli, F. Ancilotto, L. Vranješ-Markić, and J. Boronat, Phys. Rev. A **104**, 033319 (2021).

[18] A. Boudjemâa, Phys. Rev. A **97**, 033627 (2018).

[19] A. Boudjemâa, Phys. Rev. A **98**, 033612 (2018).

[20] A. Boudjemâa, K. Abbas, and N. Guebli, Atoms **10**, 64 (2022).

[21] D. M. Larsen, Ann. Phys. (Berlin) **24**, 89 (1963).

[22] F. Ancilotto, M. Barranco, M. Guilleumas, and M. Pi, Phys. Rev. A **98**, 053623 (2018).

[23] A. Griffin and H. Shi, Phys. Rep. **304**, 1 (1998).

[24] D. A. W. Hutchinson, R. J. Dodd, K. Burnett, S. A. Morgan, M. Rush, E. Zaremba, N. P. Proukakis, M. Edwards, and C. W. Clark, J. Phys. B: At., Mol. Opt. Phys. **33**, 3825 (2000).

[25] V. I. Yukalov, Ann. Phys. (NY) **323**, 461 (2008); Phys. Part. Nuclei **42**, 460 (2011).

[26] A. Boudjemâa, J. Phys. B: At., Mol. Opt. Phys. **48**, 035302 (2015).

[27] A. Boudjemâa, *Degenerate Bose Gas at Finite Temperatures* (LAP LAMBERT Academic Publishing, San Diego, CA, 2017).

[28] C. D'Errico, M. Zaccanti, M. Fattori, G. Roati, M. Inguscio, G. Modugno, and A. Simoni, New J. Phys. **9**, 223 (2007).

[29] A. Marte, T. Volz, J. Schuster, S. Dürr, G. Rempe, E. G. M. van Kempen, and B. J. Verhaar, Phys. Rev. Lett. **89**, 283202 (2002).

[30] S. Stringari and J. Treiner, Phys. Rev. B **36**, 8369 (1987).